1714–1723 *Nucleic Acids Research, 2000, Vol. 28, No. 8*

Role of RNA structure in non-homologous recombination between genomic molecules of brome mosaic virus

Marek Figlerowicz*

Institute of Bioorganic Chemistry, Polish Academy of Sciences, Noskowskiego 12/14, 61-704 Pozna, Poland

Received January 5, 2000; Revised and Accepted February 28, 2000

ABSTRACT

Brome mosaic virus (BMV) is a tripartite genome, positive-sense RNA virus of plants. Previously it was demonstrated that local hybridization between BMV RNAs (RNA–RNA heteroduplex formation) efficiently promotes non-homologous RNA recombination. In addition, studies on the role of the BMV polymerase in RNA recombination suggested that the location of non-homologous crossovers depends mostly on RNA structure. As a result, a detailed analysis of a large number of non-homologous recombinants generated in the BMV-based system was undertaken. Recombination hot-spots as well as putative elements in RNA structure enhancing non-homologous crossovers and targeting them in a site-specific manner were identified. To verify these observations the recombinationally active sequence in BMV RNA3 derivative was modified. The results obtained with new RNA3 mutants suggest that the primary and secondary structure of the sequences involved in a heteroduplex formation rather than the length of heteroduplex plays the most important role in the recombination process. The presented data indicate that the sequences proximal to the heteroduplex may also affect template switching by BMV replicase. Moreover, it was shown that both short homologous sequences and a hairpin structure have to accompany a double-stranded region to target non-homologous crossovers in a site-specific manner.

INTRODUCTION

Although the passing decade has brought remarkable progress in the studies of genetic recombination in viral RNA, the molecular mechanism of this process remains unclear. Most of the data collected from different experimental systems (*in vitro* and *in vivo*) suggest that RNA viruses recombine according to a copy-choice hypothesis (1–5). However, recently it was demonstrated that the breakage-and-ligation mechanism proved for DNA recombination can also operate during RNA recombination (6). The copy-choice hypothesis assumes that RNA recombinants are formed in result of template switching by viral replicase during genomic RNA replication (1). Depending on the primary structure of the recombining molecules and on the location of recombinant junction sites, three types of RNA recombination were distinguished: homologous, aberrant homologous and non-homologous (3).

The molecular mechanism of template switching is better recognized for events involving two homologous RNAs, when the newly synthesized nascent strand is complementary to both donor and acceptor molecules (7–9). Non-homologous recombination is more complex, since it occurs between different RNA molecules. Generated products are usually non-functional and rarely accumulate *in vivo*. Some data suggest that viral polymerases use promoter-like structures to switch from one non-homologous template to another (10–12). Other results emphasize the role of local hybridization (local heteroduplex formation) between recombining molecules (13,14) or leader sequences (15).

Brome mosaic virus (BMV), a tripartite genome, positive-sense RNA virus, was the first plant RNA virus for which genetic RNA recombination was observed (16). It was demonstrated that BMV can support the formation of all three types of recombinants: homologous (7), aberrant homologous (8) and non-homologous (17). These observations allowed the development of an efficient BMV-based non-homologous recombination system utilizing wt RNA1, wt RNA2 and various RNA3 derivatives (Fig. 1) (14). In the latter, the 3′ non-coding region was modified and then a sequence complementary to the 3′ portion of BMV RNA1 was introduced just between the modified 3′-end and coding region. This allows local RNA1–RNA3 hybridization (heteroduplex formation), which efficiently mediates non-homologous crossovers (5,14).

The proposed mechanism assumes that recombinants are formed according to a copy choice hypothesis during the synthesis of minus RNA strands (14). Viral replicase initiates at the 3′ end of wt RNA1 (RNA donor) and then the enzyme switches to RNA3 (RNA acceptor) within the heteroduplex structure. The resulting RNA3 recombinants contain the repaired 3′ non-coding region derived from wt RNA1, whereas the coding region and 5′ end are from RNA3.

Recently, we have observed that a single amino acid mutation within the core polymerase domain of BMV 2a protein inhibits non-homologous RNA recombination without affecting the frequency of homologous crossovers (18). This demonstrated that viral polymerase participates in the studied process and suggested that different mechanisms operate in homologous and non-homologous recombination. Studies involving other BMV 2a mutants confirmed that by introducing specific modifications into viral polymerase, one can influence the frequency of homologous and non-homologous recombination

*Tel: +48 61 852 8503; Fax: +48 61 852 0532; Email: marekf@ibch.poznan.pl

as well as the location and precision of homologous crossovers (19). They also suggested that a non-homologous crossover location depends mostly on RNA structure (18,19).

The undertaken analysis of the primary and secondary structure of the sequences supporting non-homologous recombination in BMV revealed that non-homologous recombination hot-spots are usually located within AU-rich regions. In addition, putative RNA structural elements that should accompany the RNA–RNA heteroduplex to target non-homologous crossovers in a site-specific manner have been identified. To verify these observations, six new RNA3 derivatives were used to demonstrate that there is no correlation between the length of the RNA–RNA heteroduplex and its recombination activity. Non-homologous recombination in BMV is affected by the primary and secondary structure of the sequences involved in heteroduplex formation. In addition, the sequences proximal to the heteroduplex may also influence template switching by the BMV replicase. Moreover, it was shown that both specifically positioned short homologous sequences and a hairpin structure have to accompany the double-stranded region to target non-homologous crossovers in a site-specific manner. In general, the presented data indicate that non-homologous RNA recombination in BMV strongly depends on both: RNA sequence and secondary structure.

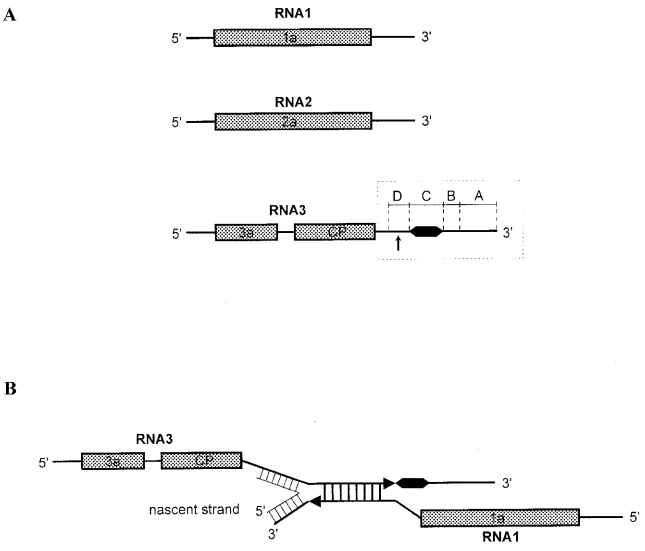

Figure 1. The BMV-based system used to study non-homologous RNA recombination in BMV. (**A**) The BMV genome (the open reading frames are boxed and labeled while the 3′ and 5′ terminal sequences are represented by lines). The genome of BMV is composed of three RNA segments: RNA1 and RNA2, which encode replicase proteins 1a and 2a, respectively, and RNA3, which encodes the movement protein (3a) and the coat protein (CP). All BMV RNAs share a highly structured 200 nt region at the 3′ end. In the BMV-based recombination system the wt RNA3 component is replaced by a derivative with the modified 3′ non-coding fragment (5′ end and coding regions are unchanged) that can be divided into regions A, B, C and D. Region A (216 nt) consists of the wt BMV RNA1 sequence (positions 1–236 from the 3′ end). Region B represents a partial duplication of region A between positions 7 and 200. Additionally, regions A and B have 20 nt deletions between positions 81 and 100. The 197 nt region C (black box) is derived from the 3′ terminal sequence of cowpea chlorotic mottle virus (CCMV) RNA3 except the last 23 nt. Region D represents a 141–30 nt RAS that is complementary to the RNA1 3′ fragment. (**B**) Schematic illustration of non-homologous recombination. Since the recombining wt RNA1 and modified RNA3 molecules contain 141–30 nt complementary sequences, they can form stable heteroduplex where crossovers occur. A newly synthesized nascent strand possesses an unmodified 3′ terminus (common for all BMV RNAs) derived from wt RNA1 whereas the coding region and 5′ end, are from RNA3.

MATERIALS AND METHODS

Materials

Plasmids pB1TP3, pB2TP5 and PN0–RNA3 are a generous gift of J. J. Bujarski (Northern Illinois University, DeKalb, IL). pB1TP3 and pB2TP5 contain full-length cDNA of BMV RNA1 and RNA2 respectively. PN0–RNA3 contains cDNA of a BMV RNA3 derivative called the recombination vector (for details see Fig. 1). Restriction enzymes (*Eco*RI, *Spe*I and *Xba*I), T7 RNA polymerase, RNasine, RQ DNase RNase free, MMLV–reverse transcriptase, *Taq* polymerase and the pUC19 cloning vector were from Promega.

Primers used for the construction of pMag0- to pMag–RNA3 plasmids (*Spe*I restriction sites are underlined): 1, 5′-ACTAGTTCGAGCAGAGGTCTCACAC-3′; 2, 5′-ACTAGTAGGTCTCACACAGAGACAAGC-3′; 3, 5′-ACTAGTAATTAAAGATCAAATCACCAGCG-3′; 4, 5′-ACTAGTCCAGCGAGCTCGCCGTTAAAGC-3′; 5, 5′-ACTAGTTCTTGTGTCGTGTTAAGGC-3′; 6, 5′-ACTAGTCATGAGGAGTACTGTTTGGTTGCC-3′; 7, 5′-ACTAGTGGGCACTACCTATAAACCGG-3′.

Primers used for a specific RT–PCR amplification of the RNA3 3′-fragment (the region where recombinants junction sites are located): first strand primer A, specific for all BMV RNAs 3′-end introducing *Eco*RI restriction site (underlined), 5′-CAGTGAATTCTGGTCTCTTTTAGAGATTTACAG-3′; and second strand primer B representing the BMV RNA3 sequence between positions 1726 and 1751, 5′-CTGAAGCAGTGCCTGCTAAGGCGGTC-3′.

Plasmid construction

To obtain pMag1–RNA3 to pMag5–RNA3 plasmids, containing cDNA of the tested BMV RNA3 derivatives, suitable fragments of RNA1 cDNA (pB1TP3) were inserted in antisense orientation into *Spe*I linearized PN0–RNA3 plasmid. All cDNA fragments were obtained by PCR for which pB1TP3 was used as a template. The following fragments of BMV RNA1 cDNA were obtained and inserted into PN0–RNA3: the 137 nt fragment between positions 2856 and 2992 (with primers 1 and 6) to make pMag1–RNA3; the 129 nt fragment between positions 2856 and 2984 (with primers 2 and 6) to construct Mag2–RNA3; the 94 nt fragment between positions 2856 and 2949 (with primers 3 and 6) to prepare Mag3–RNA3; the 77 nt fragment between 2856 and 2932 (with primers 4 and 6) to obtain Mag4–RNA3; and the 40 nt fragment between 2856 and 2895 (with primers 5 and 6) to construct Mag5–RNA3. pMag0–RNA3 was constructed in two steps. First, the 76 nt portion of PN0–RNA3 (between *Xba*I and *Spe*I restriction sites) was replaced with the 11 nt shorter fragment obtained by PCR using primers B and 7 and PN0–RNA3 as a template. In result the PN(-h)–RNA3 plasmid was obtained. In the next step the 137 nt fragment of RNA1 cDNA (previously used to obtain pMag1–RNA3) was inserted into *Spe*I linearized PN(-h) in antisense orientation. In

all cases the sequence of the pMag–RNA3 plasmids were confirmed by sequencing.

In vivo recombination assay

To test recombination activity of the Mag0–RNA3 to Mag5–RNA3 derivatives the previously described procedure was applied (14,20). Briefly, infectious molecules of BMV RNA1, RNA2 and Mag0–RNA3 to Mag5–RNA3 derivatives were obtained by *in vitro* transcription for which *Eco*RI linearized plasmids pB1TP3, pB2TP5 and Mag0–RNA3 to Mag5–RNA3 were used. Four leaves of two *Chenopodium quinoa* plants (a local lesion host for BMV) were mechanically inoculated with the mixtures containing BMV RNA1, RNA2 and one of the Mag–RNA3 derivatives. After 2 weeks, when infection symptoms were well developed, separate local lesions were excised and the total RNA was isolated. The extracted RNA was subjected to RT–PCR involving primer A (first strand primer) and primer B (second strand primer) specific for amplification of the RNA3 progenies 3′-portion (region where crossovers occur). The BMV-based recombination system was designed in such a way that generated recombinants possess visibly shorter 3′-non-coding region than parental Mag0–RNA3 to Mag1–RNA3 molecules. To determine whether recombinants were formed in infected cells, the RT–PCR products were analyzed by 1.5 % agarose gel electrophoresis and their length was compared with the length of the fragment amplified using primers A, B and Mag0–RNA3 to Mag5–RNA3 as a template. For the selected recombinants, their presence in local lesions was additionally confirmed by northern blot hybridization. Finally, RT–PCR products were cloned into the pUC19 vector and sequenced to determine recombinant junction site locations. The full experiment involving each RNA3 derivative was repeated four times.

RESULTS

Putative RNA structural elements enhancing non-homologous recombination

Two hundred and six non-homologous recombinants have been previously identified during the *in vivo* studies of genetic recombination between BMV RNAs (14,17–21) In most cases, each recombinant was isolated from a different lesion as described in Materials and Methods (only ~5% of lesions contained two, rarely three different recombinants). All recombinants raised as a result of the crossovers between wt RNA1 and modified RNA3 [10 various RNA3 derivatives named PN1(-) to PN10(-) RNA3 were used, see Fig. 2]. Recombinant junction sites were located within or in proximity to the local heteroduplexes formed by recombining molecules.

In order to identify the structural motifs involved in non-homologous recombination between BMV RNAs, the nucleotide sequences of the parental and recombinant molecules within and at the vicinity of the junction sites were assessed carefully. The analysis of recombination hot-spots revealed that some recombinants were generated more frequently than the others. This phenomenon was especially pronounced for recombinants generated with a series of five RNA3 derivatives shown in detail in Figure 3 (14). In the first PN1(-) RNA3 construct a recombinationally active region (RAS) comprised a 141 nt sequence complementary to wt RNA1 (between positions 2852 and 2992). The remaining four RNA3 derivatives [PN2(-) to PN5(-)] contained the same sequence with various deletions at the 3′-side. As a result, heteroduplexes which RNA1 was capable of forming with PN1(-) to PN5(-) RNA3 had identical left parts (the regions where crossovers were located) and different right portions (Figs 2 and 3).

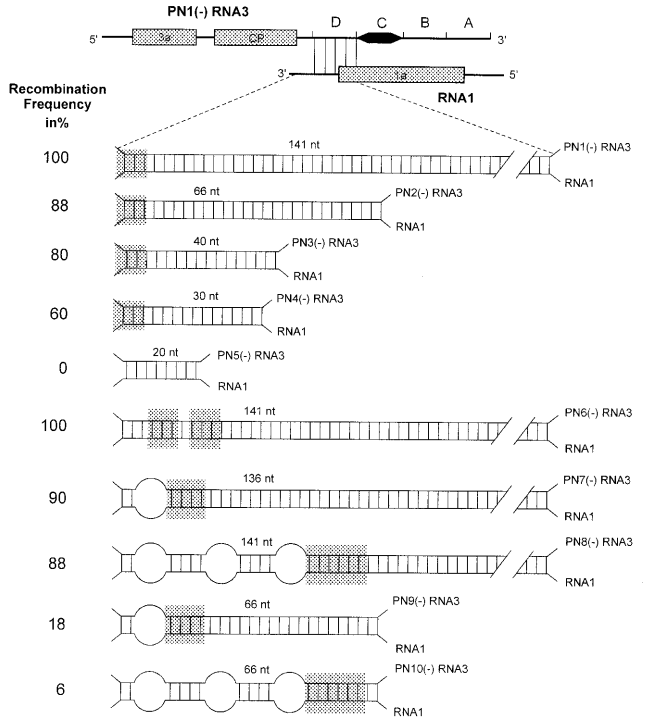

Figure 2. Schematic description of the heteroduplexes formed by wt RNA1 and PN1(-) to PN10(-) RNA3 derivatives (14). All RNA3 derivatives have the same general organization (presented in Fig. 1). In the basic construct, named PN1(-) RNA3, region D consists of a 141 nt RAS (complementary to wt RNA1 between positions 2852 and 2992), which allows local RNA1–RNA3 hybridization (hetreroduplex formation, depicted by short vertical lines at the top). To construct the remaining nine RNA3 derivatives different fragments of the RAS were removed or modified to affect the structure of RNA1–RNA3 heteroduplexes (14). To obtain PN2(-) to PN5(-) RNA3 derivatives, various 3′-portions of the RAS were deleted. In PN6(-) RNA3 several mismatches were introduced into left portion of the heteroduplex. To construct PN7(-) and PN8(-) RNA3, one and three internal loops were inserted into the local double-stranded region, respectively, while in PN9(-) and PN10(-) RNA3, a 73 nt 3′-fragment of the RAS was additionally removed. The regions where recombination crossovers most frequently occur are shaded. RF was defined as the ratio between the number of the lesions that developed recombinants to the total number of the analyzed lesions.

Recombinants generated with PN1(-) to PN5(-) RNA3 derivatives can be divided into two groups. The first group comprises the recombinants in which junction sites are located close to each other (symmetrical or almost symmetrical recombinants, for example C, D or H in Fig. 3). The second group consists of the asymmetrical recombinants with junction sites located far from each other (e.g. recombinants A, B or F in Fig. 3). Interestingly, for PN1(-) to PN4(-) RNA3 derivatives the asymmetrical recombinants were generated more frequently than symmetrical ones. Out of 20 recombinants

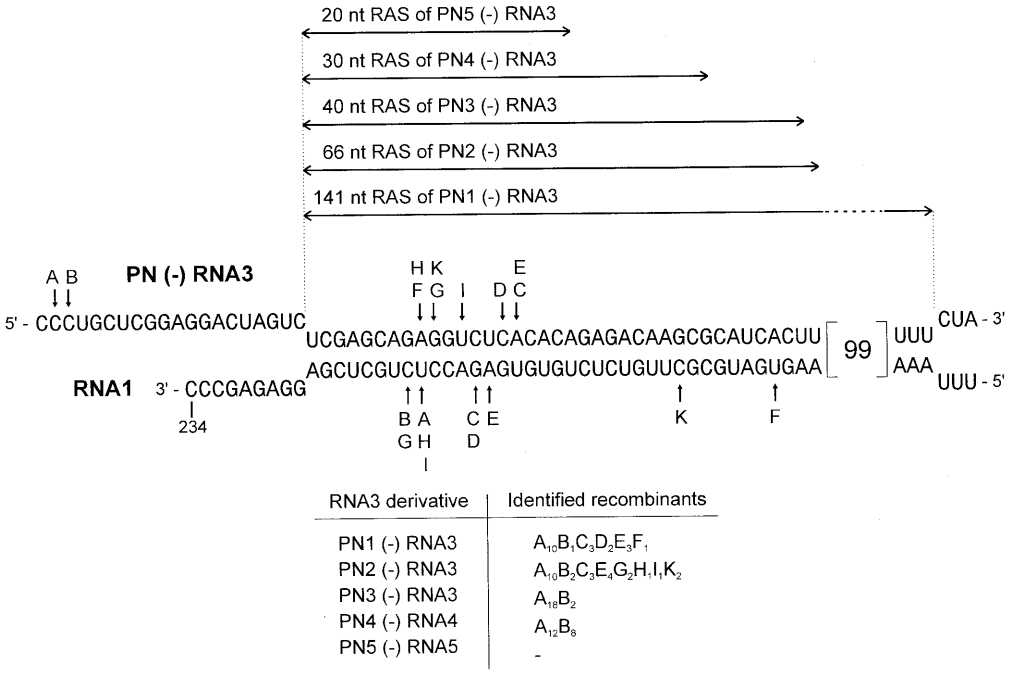

Figure 3. Non-homologous recombinants identified using PN1(-) to PN5(-) RNA3 derivatives (14). Each recombinant was isolated from a separate local lesion. The upper sequence represents the positive strand of PNx(-) RNA3 (containing the RAS complementary to RNA1), while the lower sequence represent the corresponding fragment of wt RNA1 positive strand. The recombinant junction sites are marked with arrows (pointing to the last nucleotide coming from wtRNA1 and the first nucleotide from RNA3 derivative) and with letters. Lines presented above the heteroduplex structure illustrate the length of the RAS in the individual PNx(-) RNA3 derivatives (which reflects the length of RNA1–RNA3 heteroduplex). The table below shows which recombinants (the lower index) were generated with the particular RNA3 derivative, and how frequently.

isolated for PN1(-) RNA3 12 were asymmetrical: 10 recombinants of type A and 1 recombinant of types B and F. For PN2(-) RNA3, that contained a 66 nt RAS, a similar distribution of the junction sites was observed. However, the reduction of the RAS to 40 [in PN3(-) RNA3] or to 30 nt [in PN4(-) RNA3] caused the formation of recombinants A or B exclusively (Fig. 3) (14). The latter two have the same length but they differ from each other by a single nucleotide (GU**C**U**C**C and GU**CC**CC, respectively) at the junction sites. Apparently, PN3(-) and PN4(-) RNA3 derivatives can support RNA recombination in a site-specific manner. Further shortening of the RAS to 20 nt [in PN5(-) RNA3] completely abolished the recombination process.

The RNA1 and PN1(-) to PN4(-) RNA3-derived sequences near the junction sites in recombinants A and B were studied in detail to identify which elements in RNA structure are responsible for the site-specificity of recombination. This suggested that non-homologous recombination occurs in a site-specific manner if the local RNA–RNA heteroduplex is accompanied by specifically positioned short homologous sequences (regions h in Fig. 4A). The regions h are placed in such a way that the heteroduplex formed by recombining molecules can adopt two alternative structures: either a full-length duplex or a shorter duplex followed by a hairpin on RNA3. As shown in Figure 4A, and suggested by Nagy and Bujarski (14), the formation of the hairpin brings both junction sites close to each other. This may not, however, be the only factor allowing the viral replicase to switch from one RNA template to another. The hairpin formed when viral replicase starts to penetrate RNA1–RNA3 heteroduplex may pause BMV replicase, while short homologous sequences (10–11 nt region h) generate the complementarity between the nascent strand (synthesized on the RNA1 donor) and the acceptor template.

To determine whether the same RNA structural motifs were involved in other recombinant formation the remaining recombination hot-spots found for wt RNA1 and PN1(-) to PN10(-) RNA3 were analyzed (Fig. 4B). They were located within local double-stranded regions, and generated almost symmetrical or completely symmetrical recombinants. However, only one recombinant (I) contained a short complementary sequence between the (+) nascent strand of RNA3 and (-) RNA1. The left most frequent recombinants had junction sites located close to each other within the A-U-rich regions of the heteroduplex.

In addition, the preferences of the BMV replicase to switch after certain nucleotides were investigated. This demonstrated that in 42% of recombinants a U was the last nucleotide coming from the donor template, in 30% it was an A while only in 18 and 10% it was a C or a G, respectively. Apparently, template switching by the BMV replicase most frequently occurs after nucleotides forming weaker base pairs A-U (72% of crossovers). Analogous dependence was not observed for the first nucleotide coming from the acceptor template: in 48% of recombinants it was an A or a U while in 52% of recombinants a G or a C.

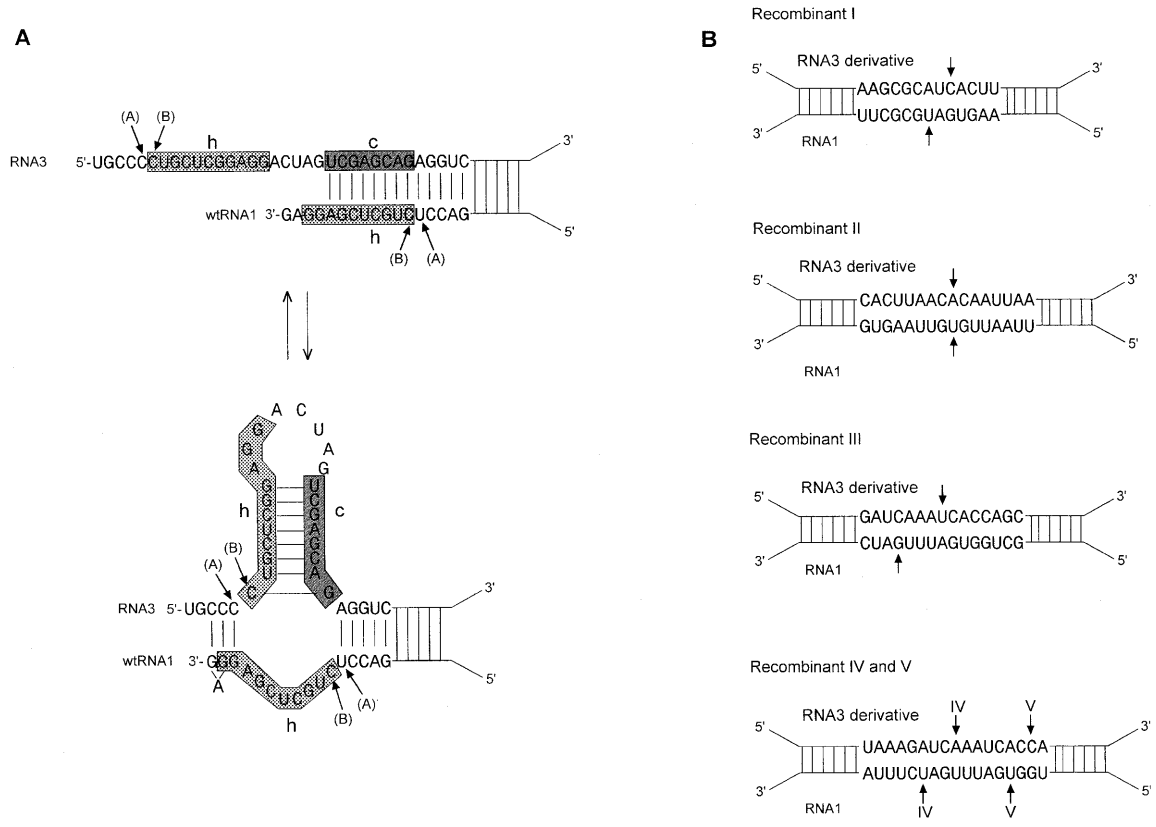

Figure 4. Putative RNA structural motifs supporting non-homologous recombination. (**A**) Site-specific non-homologous recombination. Sequences involved in site-specific recombination are highlighted, while the remaining fragment of the heteroduplex is represented by lines (the total length of the RNA1–RNA3 duplex may vary from 30 to 140 nt). Hybridization between RNA molecules is depicted by short lines. It was observed that all RNA1–RNA3 heteroduplexes mediating site-specific recombination in BMV have a common left portion that can adopt two different conformations. Recombining molecules can form a full-length duplex (the upper structure) or a shorter duplex with a hairpin on the RNA3 template (the structure below). Such structural flexibility results from the presence of short homologous sequences specifically positioned in recombining molecules (the shaded sequences marked with h). The region h is placed at the left end of the heteroduplex in RNA1 and just before the heteroduplex in RNA3. The portion of RNA3 involved either in the heteroduplex or the hairpin stem formation is shaded and marked with c. The arrows with letters indicate the junction sites of recombinants (A and B) generated as a result of site-specific crossovers. (**B**) Location of the junction sites (marked with arrows and with letters) found in recombinants that, beside A and B, were the most frequently identified during BMV infections involving PN1(-) to PN10(-) RNA3 derivatives. Local RNA1–RNA3 heteroduplexes are represented by lines and the sequences near the recombination hot-spots are highlighted.

In general, the analysis undertaken suggested that there are two different types of non-homologous recombination: site-specific, which generates asymmetrical recombinants A and B and heteroduplex-mediated, producing almost symmetrical or completely symmetrical recombinants. The first occurs if the local RNA–RNA heteroduplex is accompanied by specifically positioned short homologous sequences, while the second depends on local RNA–RNA hybridization only.

Preparation of the modified BMV RNA3 molecules

In order to obtain experimental evidence supporting the above observations, six new RNA3 derivatives serially named Mag0–RNA3 to Mag5–RNA3 were made. A basic construct Mag1–RNA3 was prepared by inserting a 137 nt RAS complementary to RNA1 (between positions 2856 and 2992) into the PN0–RNA3 recombination vector. As a result, Mag1–RNA3 and RNA1 were able to form a local double-stranded structure possessing all putative elements supporting both heteroduplex-mediated and site-specific non-homologous recombination (Fig. 5). The left portion of the RNA1/Mag1–RNA3 heteroduplex was identical as shown in Figure 4A.

To determine which elements in RNA structure mediate site-specific non-homologous recombination Mag0–RNA3 and Mag2–RNA3 derivatives were prepared. To obtain them, short deletions were introduced into Mag1–RNA3. In Mag0–RNA3, an 11 nt sequence h that lies upstream of the RAS and is homologous to the RNA1 template was removed (Fig. 5 see also Fig. 4A), while in Mag2–RNA3 the sequence that base-pairs with a portion of h (present in the donor and acceptor templates), named region c was deleted (Figs 4A and 5). In both cases, the changes introduced into Mag1–RNA3 should prevent a hairpin structure formation in the acceptor template. However, both Mag0–RNA3 and Mag2–RNA3 were able to form with RNA1, a local double-stranded region, which according to earlier data should efficiently mediate recombination crossovers (14). Mag1–RNA3 and Mag0–RNA3 formed identical heteroduplexes with RNA1, whereas the Mag2–RNA3/RNA1 duplex

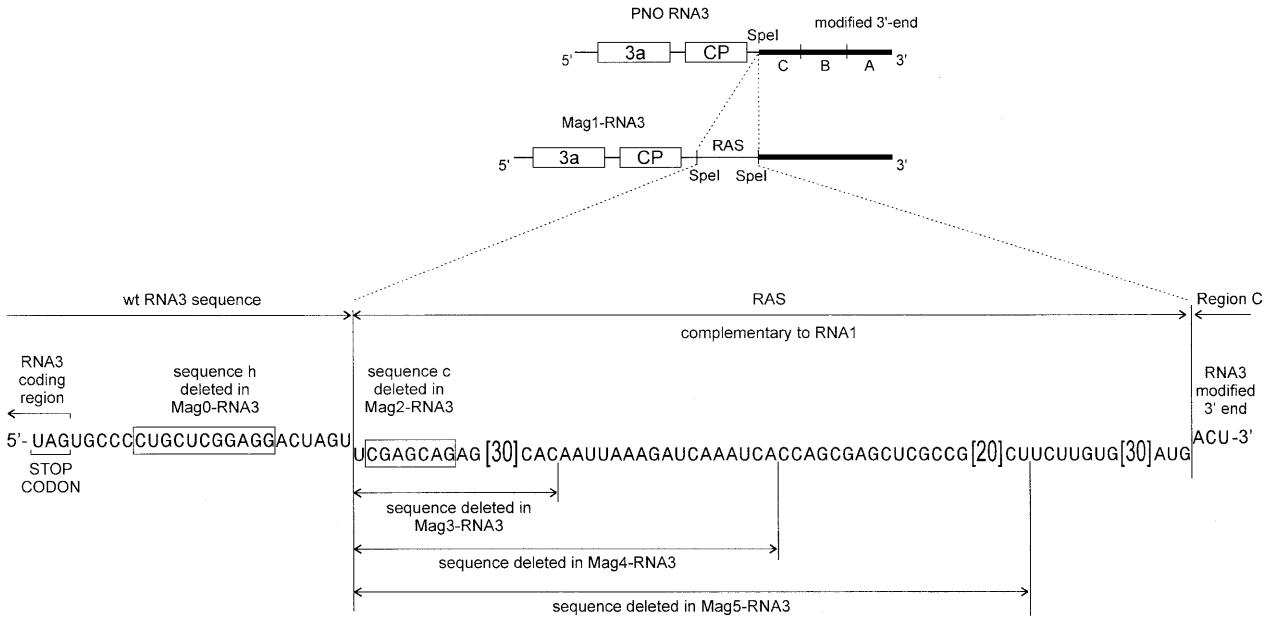

Figure 5. Schematic description of the Mag–RNA3 derivatives. To obtain Mag–RNA3 derivatives the previously described BMV recombination vector called PN0–RNA3 was applied (14). Its modified 3′ non-coding region can be divided into three regions: A, B and C. The 216 nt region A consists of the wt BMV RNA1 sequence (positions from 1 to 236 counting from the 3′-end). Region B represents a partial duplication of region A between positions 7 and 200. Additionally, A and B regions have 20 nt deletions between positions 81 and 100. The 197 nt region C is derived from the 3′ terminal sequence of CCMV RNA3 except for the last 23 nt. To obtain Mag1–RNA3, a 137 nt sequence complementary to RNA1 (RAS, highlighted at the bottom) was inserted into the recombination vector between its modified 3′-end and coding region (for details see 14). To construct the remaining five RNA3 derivatives, sequences indicated in the picture were deleted from Mag1–RNA3.

was 8 nt shorter (identical to Mag1–RNA3 formed with RNA1 when a hairpin on the RNA acceptor is present, Fig. 6).

To test how non-homologous RNA recombination is influenced by the length and structure of the sequences involved in the heteroduplex formation, various fragments of a 5′-portion of the RAS were deleted from Mag1–RNA3. This affected the left part of the RNA1–RNA3 heteroduplex, i.e. the region where recombination crossovers occurred. Resultant RNAs, Mag3–RNA3, Mag4–RNA3 and Mag5–RNA3 retained 94, 77 and 40 nt sequences of the RAS, respectively (Fig. 5). The potential heteroduplexes formed by Mag3–RNA3 and Mag4–RNA3 with RNA1 were of similar length, but the stability of their left portion should be decidedly different. Out of the first 15 bp forming the left fragment of the RNA1/Mag3–RNA3 heteroduplex 13 were A-U base pairs, while in an analogous fragment of the RNA1/Mag4–RNA3 heteroduplex 12 G-C base pairs were present. The structures of the putative heteroduplexes formed by Mag–RNA3 derivatives and RNA1 are schematically presented in Figure 6.

Recombination activity of Mag–RNA3 derivatives

The previously described recombination assay was applied to test whether modifications introduced to the Mag1–RNA3 influenced its ability to mediate RNA–RNA recombination (14,20). *Chenopodium quinoa* plants (a local lesion host for BMV) were inoculated with mixtures containing infectious, full-length transcripts of BMV RNA1, RNA2 and one of the Mag–RNA3 derivatives. After 2 weeks, the number of the lesions was counted to determine the infectivity of the tested RNA3 derivatives, individual lesions were excised and the total RNA were extracted separately from the each lesion. Then the 3′-fragment of RNA3 accumulating in every analyzed lesion was amplified by RT–PCR and the number of lesions containing recombinants was determined. In addition, the selected samples of the isolated total RNA were analyzed by northern blot hybridization to confirm that RNA3 recombinants were developed in the infected plants (data not shown).

As shown in Figure 6B, similar infection symptoms were developed for all Mag–RNA3s except for Mag3–RNA3. The latter produced a markedly reduced number of local lesions (~50% less than other RNA3 derivatives). Surprisingly, out of the tested derivatives only three: Mag1–RNA3, Mag2–RNA3 and Mag3–RNA3 supported a detectable level of recombination (100, 60 and 15% respectively). Non-homologous recombinants were not identified when either Mag0–RNA3, Mag4–RNA3 or Mag5–RNA3 was used together with RNA1 and RNA2 to inoculate plants.

To determine the structure of recombinants accumulating in local lesions the majority of RT–PCR products were cloned into the pUC19 vector and sequenced. For 10 RT–PCR products (obtained with every RNA3 derivative) several clones were sequenced to determine the number of different recombinants accumulating in an individual lesion. This confirmed earlier observations of Nagy and Bujarski that most analyzed lesions contain a single recombinant (14). Only in 5% of lesions two different recombinants were identified. Recombinant junction sites were clustered within the left portion of the heteroduplexes (Fig. 7). For Mag1–RNA3 two earlier identified

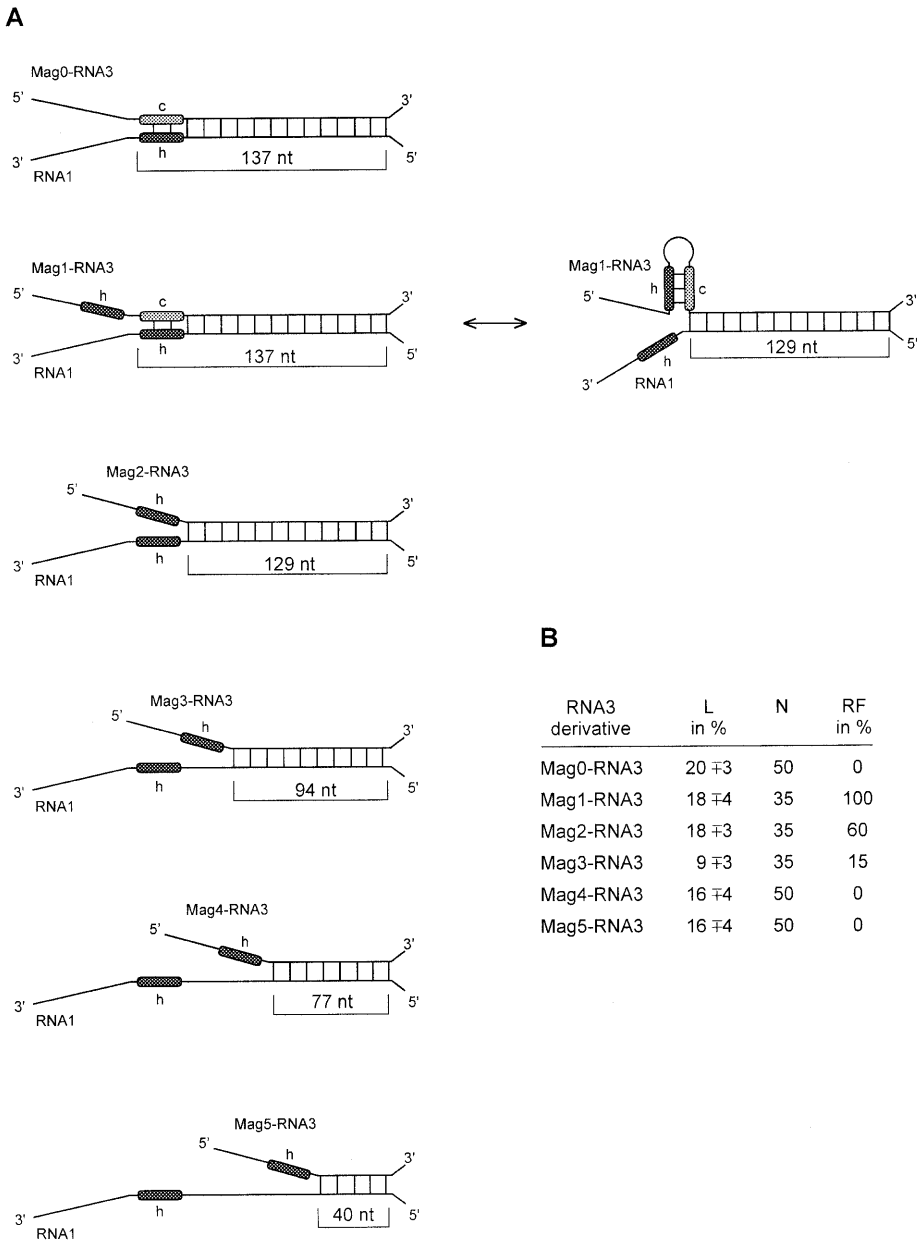

RNA3 derivative	L in %	N	RF in %
Mag0-RNA3	20 ∓3	50	0
Mag1-RNA3	18 ∓4	35	100
Mag2-RNA3	18 ∓3	35	60
Mag3-RNA3	9 ∓3	35	15
Mag4-RNA3	16 ∓4	50	0
Mag5-RNA3	16 ∓4	50	0

Figure 6. Recombination activity of the Mag–RNA3 derivatives. (**A**) Schematic description of the heteroduplexes whose Mag–RNA3 derivatives can potentially form with RNA1. Solid lines represent the donor and acceptor templates. The short sequences involved in site-specific recombination are boxed (regions h and c). The short vertical lines symbolize local hybridization between recombining molecules. The left portion of the local double-stranded region formed by Mag1–RNA3 and RNA1 is exactly the same as the one shown in Figure 4A. For that reason, the RNA1/Mag1–RNA3 heteroduplex can exist in two different conformations: as a full-length duplex (left) or as a shorter duplex followed by a hairpin on the acceptor template (right). Sequence h was removed from Mag0–RNA3 and so this acceptor template can only form a full-length duplex with RNA1. In the Mag2–RNA3 derivative, sequence c was deleted. As a result Mag2–RNA3 and RNA1 can only form the shorter duplex (identical to Mag1–RNA3 when the hairpin structure is present). The duplexes formed by three other RNA3 derivatives: Mag3–RNA3, Mag4–RNA3 and Mag5–RNA3 are decidedly shorter. (**B**) Influence of the Mag–RNA3 derivatives on RF observed during infection in *C.quinoa* plants (plants were inoculated with mixtures containing BMV RNA1, RNA2 and one of the Mag–RNA3 derivatives). The number of local lesions developed on *C.quinoa* leaves was counted to characterize the infectivity of the Mag–RNA3 derivatives, (L, average number of the lesion per leaf). RF was defined as the ratio between the number of the lesions that developed recombinants to the total number of the analyzed lesions (N).

types of recombinants were observed: nearly symmetrical (with both junction sites located within the double-stranded region, e.g. C, D or E in Fig. 7) and asymmetrical (for which one of the junction sites was located within heteroduplex on RNA1, while another was placed just before the double-stranded region on the RNA3 derivative, e.g. A and B). As for PN1(-) and PN2(-) RNA3, recombinant A was formed more frequently than others. Earlier it had been identified as being

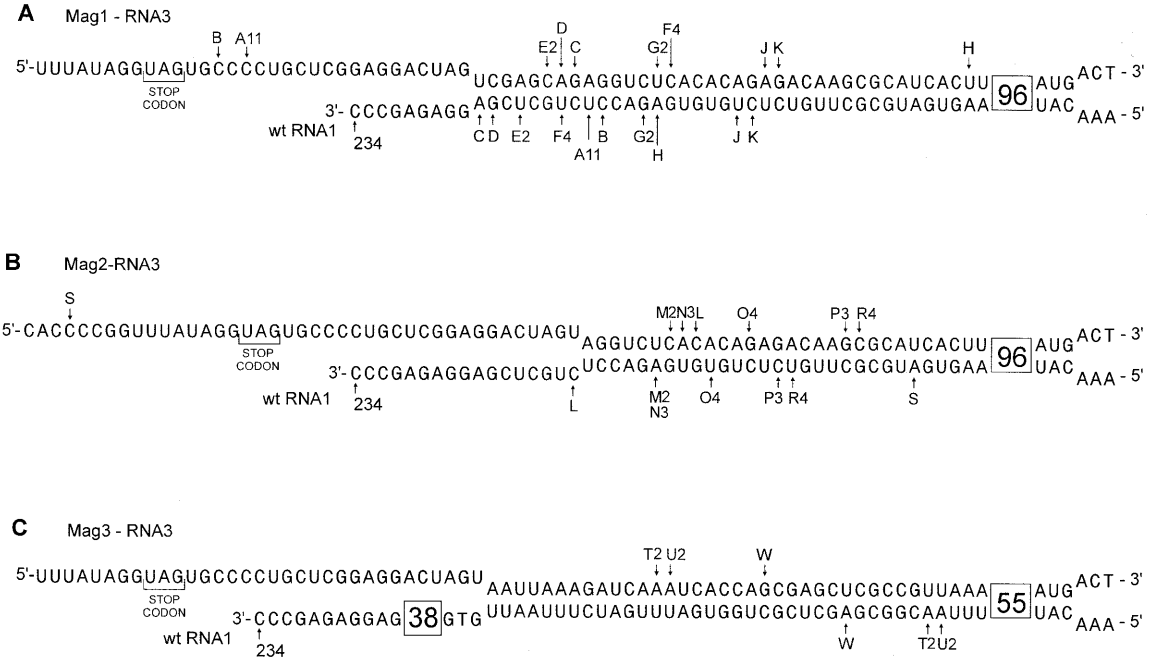

Figure 7. Distribution of the non-homologous crossovers occurring *in vivo* between BMV RNA1 and Mag1–RNA3 (**A**), Mag2–RNA3 (**B**) and Mag3–RNA3 (**C**). Each recombinant was isolated from a separate local lesion. The upper sequence represents the (+) strand of Mag–RNA3 (the region where RAS is located) while the lower sequence represents the corresponding (complementary) fragment of the (+) RNA1 strand. The recombinant junction sites are marked with arrows (pointing to the last nucleotide coming from wtRNA1 and the first nucleotide from the RNA3 derivative) and with capital letters. Numbers accompanying the letters indicate how often the given recombinant was identified.

generated as the result of site-specific non-homologous recombination. Practically, only the first type of recombinants (nearly symmetrical ones) was detected for two other RNA3 derivatives supporting recombination, i.e. Mag2–RNA3 and Mag3–RNA3. Exclusively in recombinant S (generated with Mag2–RNA3) junction sites were arranged in a different manner. Recombinant S was unlike the other also for the reason that one of its junction sites was located in the RNA3 coding region and therefore it encoded mutated coat protein. The last five amino acids of the coat protein (counting from the C-terminus) Thr-Pro-Val-Tyr-Arg-Stop were replaced by six new ones followed by a stop codon His-Ala-Leu-Val-Ser-Val-Stop. In spite of this, recombinant S accumulated in infected plants to a similar level as other recombinants.

DISCUSSION

Structural elements supporting site-specific non-homologous recombination

Mag1–RNA3 derivative was prepared in such a way that it should support both heteroduplex-mediated and site-specific non-homologous recombination. The analysis of the recombinants formed with PN1(-) to PN5(-) RNA3 suggested that site-specific crossovers (resulting in recombinant A or B formation) depend on the presence of short homologous sequences, which accompany local RNA–RNA heteroduplex (Fig. 4A). Indeed, it was observed that the deletion of region h from Mag1–RNA3 (in Mag0–RNA3) completely inhibited recombinant A or B formation. One can speculate that recombinants A and B were generated according to a mechanism operating in homologous recombination. This is contradicted, however, by the fact that Mag2–RNA3, in which sequence c was removed (to prevent hairpin formation), did not support recombinant A and B formation although it possessed the same sequence homologous to RNA1 as Mag1–RNA3 (Figs 5 and 6). For Mag2–RNA3, which formed with RNA1 the 129 nt heteroduplex, recombination frequency (RF) was reduced to 60%. In all identified recombinants (except S), both junction sites were located within a double-stranded region.

Altogether, this indicates that all three elements, i.e. the heteroduplex structure, short homologous sequences and a hairpin on RNA3 (which forms when the BMV replicase unwinds a few first base pairs of the heteroduplex) are required to target non-homologous crossovers in a site-specific manner. Basing on the presented data the following mechanism of site-specific non-homologous recombination is proposed (Fig. 8). BMV replicase initiates nascent strand synthesis at the RNA1 3′-end. The (-) RNA strand synthesis is paused when the replication complex starts to unwind the heteroduplex structure inducing a stable hairpin formation on the acceptor template. The BMV replicase may pause because of strong donor–acceptor hybridization or because of a hairpin formation on RNA3. At the same time, local hybridization ensures that the acceptor template is close enough to the pausing site. Thereafter, viral replicase and the 3′ end of the nascent strand are released from the donor

template (as a complex or separately), while the remaining portion of the nascent RNA is still hybridized to RNA1. Then the regeneration of the full-length heteroduplex can cause the re-annealing of the replicase-nascent strand complex on RNA1 to be difficult. Instead, the complex can land within the homologous region on the acceptor template (the region which is not engaged in heteroduplex formation) and the nascent strand elongation can be reinitiated on RNA3.

Surprisingly, the deletion of region h in Mag0–RNA3 completely inhibited recombination indicating that in some cases even a very long heteroduplex does not mediate non-homologous crossovers. In addition, this reveals that region h is somehow involved in the formation of the nearly symmetrical recombinants observed for Mag1–RNA3 (recombinants in which both junction sites are located within the heteroduplex structure). Such a result suggests that sequences at the vicinity of the heteroduplex may also influence the recombination process. One may speculate that Mag0–RNA3 does not support recombination since its sequence has been modified close to the stop codon for the coat protein ORF, where *cis*-acting sequence for RNA3 may be present. However, this is most likely not the case, since lacking region h Mag0–RNA3 was infectious and accumulated to a similar level to other Mag–RNA3 derivatives (except Mag3–RNA3 for which reduced infectivity was observed). Moreover, the deleted region h can be restored by recombination as it is observed for well accumulating recombinants A, B or S (where sequence h is derived from the donor template).

Role of the heteroduplex structure

The influence of the length of the RNA1–RNA3 heteroduplex on the frequency of non-homologous crossovers between BMV RNAs was previously tested by Nagy and Bujarski (14). The studies involved nine RNA3 derivatives: PN1(-) to PN5(-) RNA3 (presented earlier in detail in Figs 2 and 3) and PN7(-) to PN10(-) RNA3 (shown schematically in Fig. 2). PN7(-) and PN8(-) RNA3 could form similar heteroduplexes with RNA1 as PN1(-) RNA3 did. However, in both cases internal loops were introduced within the left portion of the local double-stranded regions to disrupt its stability [one loop in PN7(-) RNA3 and three loops in PN8(-) RNA3]. In PN9(-) and PN10(-) RNA3 a 73 nt 3′-fragment of the PN7(-) and PN8(-) RNA3 RAS, respectively, was deleted. As a result, the former two were capable of forming heteroduplexes of a similar length to the RNA1/PN2(-) RNA3 heteroduplex (14). PN7(-) and PN8(-) RNA3 supported non-homologous crossovers at the same level as PN1(-) RNA3 while for PN9(-) and PN10(-) RNA3 RF was reduced to 18 and 6% respectively. Additionally, heteroduplex destabilization shifted recombinant junction sites 30–80 nt downstream on the RNA3 and 30–60 nt upstream on RNA1 (14).

In current studies almost the same RAS as present in PN1(-) RNA3 was tested, but this time its left portion was modified. The results obtained for Mag1–RNA3 confirmed the former data achieved with PN1(-) and PN2(-) RNA3 (14), since all three RNA3 derivatives display the same recombination activity and mediate similar recombinant formation. For PN1(-) and PN2(-) RNA3, asymmetrical recombinants A and B were also generated most frequently (especially A), while the symmetrical or nearly symmetrical recombinants were located in the same region (14). This changed with other Mag–RNA3 derivatives. Shortening the RAS to 94 nt in Mag3–RNA3 drastically reduced RF to 15%. At the same time, Mag4–RNA3 and Mag5–RNA3 capable of forming 77 and 40 nt hetero-duplexes did not support recombination crossovers. These data may suggest that a relatively long heteroduplex (~100 nt) is

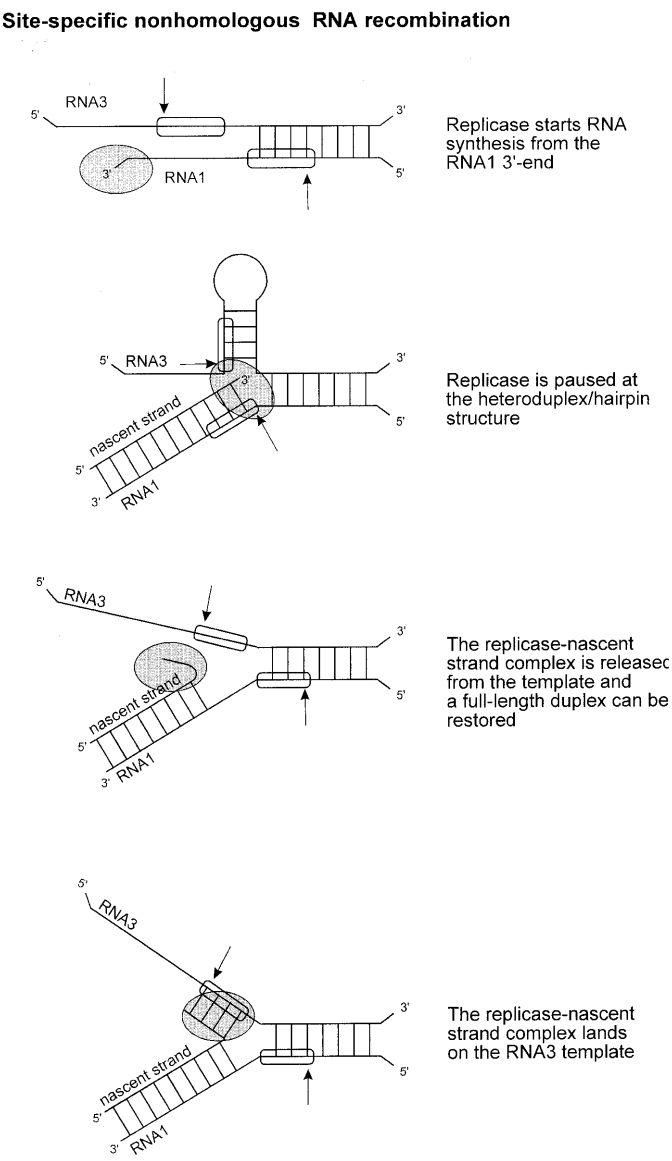

Figure 8. Schematic description of the proposed mechanism of site-specific recombination between BMV RNAs. Solid lines represent RNA1, RNA3 and nascent strand molecules. Thin vertical lines show local RNA hybridization, while the shaded oval symbolizes the viral replicase. Short homologous sequences h which accompany the heteroduplex structure are boxed. Arrows indicate the location of recombinant junction sites. The individual steps of template switching by BMV replicase are described in the figure. Briefly, the model postulates that RNA synthesis begins at the 3′-end of the donor template (RNA1). The nascent RNA strand synthesis is paused when the replication complex starts to unwind the heteroduplex structure inducing a stable hairpin formation on the acceptor template (RNA3). Thereafter, the replicase and nascent strand are released from the donor separately or as a complex. During the next stage, the 3′-end of the nascent strand hybridizes to sequence h located on the acceptor template, and the replicase reinitiates RNA synthesis.

required to mediate non-homologous recombination between BMV RNAs. However, in combination with earlier Nagy and Bujarski's results (14) they demonstrate that there is no simple correlation between the length of the heteroduplex structure and its ability to mediate recombination crossovers.

These results raise the interesting question of why were PN1(-) to PN4(-) RNA3 supporting a very high level of non-homologous recombination (from 100 to 60%, practically regardless of the heteroduplex length) (14), whereas recombination was infrequent or absent for Mag3–RNA3, Mag4–RNA3 and Mag5–RNA3 capable of forming 40–90 bp heteroduplexes? It is likely that the primary and/or secondary structure of the sequences involved in the heteroduplex formation affects its ability to induce non-homologous crossovers. A similar phenomenon was observed for homologous recombination between BMV RNAs, where the relative location of AU- and GC-rich sequences induced or inhibited crossovers within region of local homology between RNA2 and RNA3 (8,9).

In fact, the observations presented above indicate that the BMV replicase preferably switches within AU-rich portions of the heteroduplex. The left part of the RNA1/Mag3–RNA3 heteroduplex is an example of such an AU-rich region, correlating with the ability of Mag3–RNA3 to induce recombination crossovers. Furthermore, Mag4–RNA3 possessing a GC-rich 5′-fragment of the RAS was unable to induce recombination, although earlier results demonstrated that recombinants, which can potentially form during infection with Mag4–RNA3, accumulate to a similar level as the other [e.g. recombinants generated with PN8(-) RNA3 were shifted 30–80 nt downstream on the RNA3] (14,18–22). On the other hand high recombination activity of the PN1(-) to PN4(-) RNA3 derivatives may result from the fact that all of them have an identical left fragment, where sequences supporting site-specific recombinations are located. Out of 85 recombinants identified for PN1(-) to PN4(-) RNA3, 50 were of type A and 13 of type B (14). In addition to heteroduplex, two elements in the RNA structure are required to generate them; therefore only 22 left recombinants (non-A and non-B) can be classified as products of heteroduplex-mediated recombination. Thus it seems that the primary and/or secondary structure of the sequences involved in heteroduplex formation rather than the length of the heteroduplex plays the most important role in the recombination process.

Mechanism of non-homologous RNA recombination between BMV RNAs

The data presented in this article have allowed the proposition of the putative mechanism of site-specific non-homologous recombination (Fig. 8). However, these results cannot precisely explain the formation of recombinants with both junction sites located within the heteroduplex (heteroduplex-mediated crossovers). One may assume that they are also formed according to a copy-choice mechanism. During the first stage, the replication complex could pause because of strong donor–acceptor hybridization. But it still remains unclear how the viral replicase and the nascent strand are transferred from one template to another, and which elements in RNA and/or protein structure can mediate such a process (especially for recombinants in which junction sites are located far from each other within the heteroduplex structure). The data presented strongly suggest that donor–acceptor hybridization itself does not always ensure template switching by viral replicase. Non-homologous RNA recombination also depends on the primary and secondary structure of the hybridized sequences as well as sequences proximal to the heteroduplex.

On the other hand, it cannot be excluded that heteroduplex-mediated recombination occurs by RNA breakage and rejoining. This opinion is supported by the fact that similar to splicing, heteroduplex-mediated recombination depends on RNA secondary structure. Additionally, recombination crossovers are clustered within AU-rich regions that are especially susceptible to breakage (23,24); an A-U phosphodiester bond is about 50 times less stable than a C-G and 100 times less stable than a G-G. Therefore, further studies are required to demonstrate whether the same or different mechanisms operate in heteroduplex-mediated and site-specific non-homologous RNA recombination.

ACKNOWLEDGEMENTS

The author would like to thank Jozef J. Bujarski of Northern Illinois University for helpful comments and discussion. This research was supported by the Polish Government through a grant (6P04A 02712) from the State Committee for Scientific Research (KBN).

REFERENCES

1. Nagy,P.D. and Simon,A.E. (1997) *Virology*, **235**, 1–9.
2. Kirkegaard,K. and Baltimore,D. (1986) *Cell*, **47**, 433–443.
3. Lai,M.M.-C. (1992) *Microbiol. Rev.*, **56**, 61–79.
4. Saimon,A.E. and Bujarski,J.J. (1994) *Annu. Rev. Phytopathol.*, **32**, 337–361.
5. Bujarski,J.J. and Nagy,P.D. (1996) *Semin. Virol.*, **7**, 363–372.
6. Chetverin,A.B., Chetverina,H.V., Demidenko,A.A. and Ugarov,V.I. (1997) *Cell*, **88**, 503–513.
7. Nagy,P.D. and Bujarski,J.J. (1995) *J. Virol.*, **69**, 131–140.
8. Nagy,P.D. and Bujarski,J.J. (1996) *J. Virol.*, **70**, 415–426.
9. Nagy,P.D. and Bujarski,J.J. (1997) *J. Virol.*, **71**, 3799–3810.
10. Cascone,P.J., Haydar,T.F. and Simon,A.E. (1993) *Science*, **260**, 801–805.
11. Carpenter,C.D., Oh,J.-W., Zhang,C. and Simon,A.E. (1995) *J. Mol. Biol.*, **245**, 608–622.
12. Nagy,P.D., Zhang,C. and Simon,A.E. (1998) *EMBO J.*, **17**, 2392–2403.
13. Romanova,L.I., Blinov,V.M., Tolskaya,E.A., Victorova,E.G., Kolesnikova,M.S., Guseva,L.A. and Agol,V.I. (1986) *Virology*, **155**, 202–213.
14. Nagy,P.D. and Bujarski,J.J. (1993) *Proc. Natl Acad. Sci. USA*, **90**, 6390–6394.
15. Zhang,X. and Lai,M.M.-C. (1994) *J. Virol.*, **68**, 6626–6633.
16. Bujarski,J.J. and Kaesberg,P. (1986) *Nature*, **321**, 528–531.
17. Bujarski,J.J. and Dzianott,A.M. (1991) *J. Virol.*, **65**, 4153–4159.
18. Figlerowicz,M., Nagy,P.D. and Bujarski,J.J. (1997) *Proc. Natl Acad. Sci. USA*, **94**, 2073–2078.
19. Figlerowicz,M., Nagy,P.D., Tang,N., Kao,C.C. and Bujarski,J.J. (1998) *J. Virol.*, **72**, 9192–9200.
20. Nagy,P.D. and Bujarski,J.J. (1992) *J. Virol.*, **66**, 6824–6828.
21. Nagy,P.D., Dzianott,A., Ahlquist,P. and Bujarski,J.J. (1995) *J. Virol.*, **69**, 2547–2556.
22. Bujarski,J.J. and Nagy,P.D. (1994) *Arch. Virol.*, **9**, 231–238.
23. Kierzek,R. (1992) *Nucleic Acids Res.*, **20**, 5073–5077.
24. Kierzek,R. (1992) *Nucleic Acids Res.*, **20**, 5079–5084.